Computational Mechanics 24 (2000) 476–490 © Springer-Verlag 2000

A localized version of the method of Lagrange multipliers and its applications

K. C. Park, C. A. Felippa, U. A. Gumaste

Abstract This paper describes a novel version of the method of Lagrange multipliers for an improved modeling of multi-point constraints that emanate from contact-impact problems, partitioned structural analysis using parallel computers, and structural inverse problems. It is shown that the classical method of Lagrange multipliers can lead to a non-unique set of constraint conditions for the modeling of interfaces involving more than two or multi-point substructural interface nodes. The proposed version of the method of Lagrange multipliers leads not only to unique construction of constraints but also encounters no singularity in modeling an arbitrary number of multi-point constraints. An important utilization of the present method is in the regularized modeling of interfaces whose rigidities are radically different from one to another. The present approach is demonstrated via several examples for its simplicity in modeling constraints, ease of implementation and computational advantages.

1 Introduction

This article presents a novel version of the method of Lagrange multipliers that is simple to formulate and implement for the modeling of multi-point constraints that emanate from contact-impact problems, partitioned solution of finite element systems, and inverse problems. Even though the method has been widely used in constraint modeling, several versions of this method arise depending on the way interface constraints are constructed. This in turn greatly influences computational strategies.

The classical version comes straight from Lagrange. His original motivation was to derive the equilibrium equations of a system of constrained rigid bodies. Lagrange treated the problem "as if all bodies are entirely free" and formulated the virtual work by summing up the contributions of "entirely free" individual bodies. He then identified the "equations of condition" [that is, the equality constraint equations] among the kinematic differential variables. Once identified, each constraint equation was multiplied by an indeterminate coefficient and added to the virtual work of the free bodies to yield the total virtual work of the system. He states: "the sum of all the terms which are multiplied by the same differential [same variation in modern usage] are equated to zero, which will give as many particular solutions as there are differentials. . . . These equations, being then rid of the indeterminate coefficients by elimination, will provide all of the conditions necessary for equilibrium." (Lagrange, 1788; Lanczos, 1970; Dugas, 1988).

We observe that the Lagrange multipliers that were introduced so that the principle of virtual work is applicable to model systems of interconnected components, are in the end eliminated. Physically, this means that once the individual components are assembled, the interaction forces cancel one another due to Newton's 3rd law. Therefore, regardless of how one constructs the constraints the resulting equilibrium equations that are free from the unknown reactions become a unique minimum set of equilibrium equations as long as there is no redundancy in the constraint equations. In other words, the final minimum set of equilibrium equations is independent of the way constraints are constructed. Mach (1960) characterized Lagrange's introduction of multipliers "the economy of science in analytical mechanics. This is echoed in Routh (1905), "Our object is to form the general equations of motion of a dynamical system free from all unknown reactions,. . .,. In order to eliminate reactions we shall use the principle of virtual work [with indeterminate multipliers]."

Over the past several decades, there has been a steady shift away from elimination toward retaining of the Lagrange multipliers in the formulation of constrained mechanical and structural systems. This shift has been largely influenced by computational considerations in multibody dynamics (Likins, 1970; Haug, 1984), parallel computations (Farhat and Roux, 1991, 1994), and recently structural inverse problems (Park, Reich and Alvin 1997). When each of the "entirely free" individual bodies or substructures is constrained to only one other body, the classical method of Lagrange multipliers (hereafter called the classical λ-method) yields a straightforward formulation. That is, add up the virtual work of individual bodies to obtain the total virtual work of entirely free bodies (e.g., an open chain link), multiply each of the kinematic

Received November 1998

K. C. Park, C. A. Felippa, U. A. Gumaste
Department of Aerospace Engineering Sciences
and Center for Aerospace Structures, University of Colorado,
Campus Box 429, Boulder, CO 80309

The present research has been supported by the National Science Foundation under a grant High Performance Computer Simulation of Multiphysics Problems (Grant Number ECS-9725504), by Sandia National Laboratories under Accelerated Strategic Computational Initiative (ASCI) Contract AS-5666, and ASCI/Level-II Contract with Lawrence Livermore National Laboratory (Contract B347880).

constraints between any two bodies or two adjacent nodes by the Lagrange multiplier vector and append one by one to the total virtual work of the system. The stationarity of the resulting constrained virtual work yields the system equilibrium equations in terms of the displacements of the "entirely free" individual bodies and the Lagrange multipliers. For this case the constraint is uniquely constructed, leading to a unique set of Lagrange multipliers.

When a node in a substructure is connected to more than one body, however, the uniqueness in the construction of corresponding constraints is lost, often yielding a redundant set of constraints. While such redundancy can be eliminated by employing a judicious constraint construction procedure or via a rank search algorithm, it does not in general offer the so-called *one-to-one duality* between the interface nodal displacements and the corresponding Lagrange multipliers with the exception of a single chain link. In other words, the physical interface forces consist of a linear combination of the Lagrange multipliers.

The objective of the present paper is to describe an alternative modeling of constraints which offers: a unique way of constructing constrains without any redundancy; the one-to-one-duality between the interface displacements and the corresponding Lagrange multipliers that possess the physical interface force; and, an ability of regularizing a flexibility mismatch when bodies of radically different rigidities are brought into assembly or contact.

2
Review of the classical method of Lagrange multipliers

This section illustrates the two difficulties alluded to in the Introduction, one pertaining to unique constraint construction and the other computational issues.

2.1
Non-uniqueness in constraint construction

Consider *partitioning* the assembled system (Fig. 1a) into 4 components, which gives rise to reaction forces along the partition boundaries. One option is to partition body 1 first from bodies 2, 3 and 4 as shown in Fig. 1b. Note it is not physically adequate for body 1 to separate away from, e.g., body 2. This gives rise to 3 kinematic constraints:

$$\begin{aligned} c_{12} &= \mathbf{u}_1 - \mathbf{u}_2 = 0 \\ c_{13} &= \mathbf{u}_1 - \mathbf{u}_3 = 0 \\ c_{14} &= \mathbf{u}_1 - \mathbf{u}_4 = 0 \end{aligned} \tag{1}$$

where the double subscripts in the constraint equation $c_{ij} = 0$ implies that the displacement of body i to be equal to that of body j.

Partitioning body 2 from bodies 3 and 4 yields two additional constraints (Fig. 1c):

$$c_{23} = \mathbf{u}_2 - \mathbf{u}_3 = 0 \quad c_{24} = \mathbf{u}_2 - \mathbf{u}_4 = 0 \tag{2}$$

Finally, partitioning body 3 from body 4 requires (Fig. 1d):

$$c_{34} = \mathbf{u}_3 - \mathbf{u}_4 = 0 \tag{3}$$

The virtual work of the "entirely free" 4 bodies is expressed as

$$\begin{aligned} W(\mathbf{u}) &= W_1(u_1) + W_2(u_2) + W_3(u_3) + W_4(u_4) \\ &= \sum_{i=1}^{N_s} W_i(\mathbf{u}_i) \end{aligned} \tag{4}$$

where $W_i(\mathbf{u}_i)$ is the virtual work of "entirely free" body i, and N_s is the number of partitioned substructures.

The constraints given in (1)–(3) lead to the following constraint functional

$$\pi_{cl}(\mathbf{u}, \lambda_{cl}) = \sum_{i=1}^{m-1} \sum_{j>i}^{m} c_{ij}\ \lambda_{ij} \tag{5}$$

where subscript (cl) refers to the classical method of Lagrange multipliers, and $m = 4$ is the number of interface nodes constrained at a same node. This is an elegant and general treatment at the cost of introducing an additional unknown for each constraint, namely λ_{ij} for each $c_{ij} = 0$. Physically, it is the reaction force between the two bodies when they are partitioned. The amazing fact is that λ_{12} appears linearly, regardless of how nonlinear the constraint is in the kinematic variables.

The total energy functional of the system is thus given by augmenting the constraint functional (5) to the virtual work:

$$\begin{aligned} \Pi(\mathbf{u}, \lambda_{cl}) &= W(\mathbf{u}) + \pi_{cl}(\mathbf{u}, \lambda_{cl}) \\ &= \sum_{i=1}^{N_s} W_i(\mathbf{u}_i) + \sum_{i=1}^{m-1} \sum_{j>i}^{m} c_{ij}\ \lambda_{ij} \end{aligned} \tag{6}$$

While the constraints resulted from the three successive partitioning steps are physically sensible, they lead to mathematical redundancies. This is because c_{23}, c_{24}, c_{34} in (2) and (3) are obtained as linear combinations of (1):

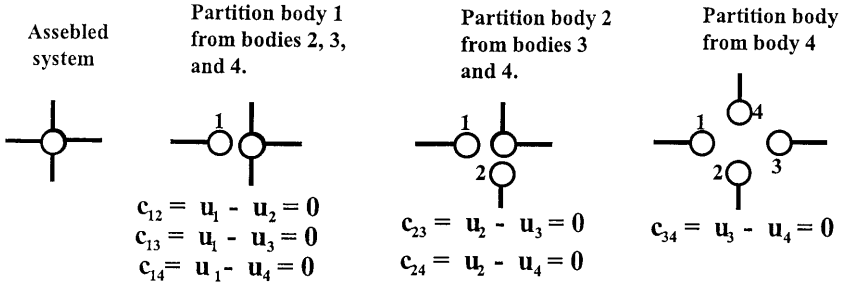

Fig. 1. Partitioning of 4 bodies

$$c_{23} = c_{13} - c_{12}, \quad c_{24} = c_{14} - c_{12}, \quad c_{34} = c_{14} - c_{13} \tag{7}$$

Thus, a rank-sufficient form of (6) is given by

$$\Pi(\mathbf{u}, \lambda_{\text{cl}}) = \sum_{i=1}^{N_s} W_i(\mathbf{u}_i) + c_{12}\ \lambda_{12} + c_{13}\ \lambda_{13} + c_{14}\ \lambda_{14} \tag{8}$$

Remark 2.1: There are several ways of partitioning. For example, one may initiate partitioning by separating body 2 from bodies 1, 3 and 4. In other words, partitioning process is non-unique.

Remark 2.2: There are a total of 6 constraints that emanate from the 4-body partitioning. However, only any three of them are linearly independent. For example, partitioning of body 1 from bodies 2, 3 and 4 is all that is necessary to yield the three independent constraints. If body 2 is partitioned first from the rest of the three bodies, then the resulting three constraints are different, implying that the Lagrange multipliers would have different physical properties.

Remark 2.3: For 10-body partitioning, there are a total of 45 possible constraints yet only 9 are linearly independent. In the partitioned analysis of 3D continua, such high connectivities are not uncommon. In addition, the impact of different choices of rank-sufficient constraint sets on computational efficiency and accuracy is not fully understood. This is especially true for contact enforcement of multiple elements being constrained.

Remark 2.4: If one chooses the three constraints emanating from the partitioning of body 1 from bodies 2, 3 and 4, the resulting constraint functional reads:

$$\pi_{\text{cl}}(\mathbf{u}, \lambda_{\text{cl}}) = \lambda_{12}(u_1 - u_2) + \lambda_{13}(u_1 - u_3) + \lambda_{14}(u_1 - u_4) \tag{9}$$

where the double subscripts are introduced in the Lagrange multipliers to emphasize the fact that they are common to the two interface nodes. For example, λ_{12} constrains the two displacement u_1 at node 1 and u_2 at node 2 to be the same. In other words, the classical Lagrange multipliers are inherently global.

Remark 2.5: Finally, we note that the very task of selecting a set of linearly independent Lagrange multipliers has been a major issue in the classical force method (Argyris and Kelsey, 1960; Denke, 1962; Przemieniecki, 1968; Patnaik, 1973; Kaneko et al., 1982; Felippa, 1987; Gallagher, 1987; Felippa and Park, 1997).

2.2 Computational issues using the classical λ-method

Let us now consider the partitioned four-spring system given by Fig. 2. In terms of virtual work approach, the total energy of the partitioned system in terms of partitioned deflection $\mathbf{u}$ and the Lagrange multiplier λ_{cl} can be expressed as (see, e.g., Lanczos, 1970):

$$\Pi(\mathbf{u}, \lambda_{\text{cl}}) = \mathbf{u}^{\text{T}}\left(\frac{1}{2}\,\mathbf{K}\,\mathbf{u} - \mathbf{f}\right) + \lambda_{\text{cl}}^{\text{T}}\,\mathbf{C}_{\text{cl}}^{\text{T}}\,\mathbf{u}$$

$$\mathbf{K} = \begin{bmatrix} k_1 & 0 & 0 & 0 \\ 0 & k_2 & 0 & 0 \\ 0 & 0 & k_3 & 0 \\ 0 & 0 & 0 & k_4 \end{bmatrix},$$

$$\mathbf{C}_{\text{cl}} = \begin{bmatrix} 1 & -1 & 0 & 0 \\ 0 & 1 & -1 & 0 \\ 0 & 0 & 1 & -1 \end{bmatrix} \tag{10}$$

$$\mathbf{u} = \begin{Bmatrix} u_1 \\ u_2 \\ u_3 \\ u_4 \end{Bmatrix}, \quad \lambda_{\text{cl}} = \begin{Bmatrix} \lambda_{12} \\ \lambda_{23} \\ \lambda_{34} \end{Bmatrix}, \quad \mathbf{f} = 0.25\begin{Bmatrix} f_1 \\ f_2 \\ f_3 \\ f_4 \end{Bmatrix}$$

where we have used Option 1 shown in Fig. 2b in order to secure a linearly independent system. The stationarity of the constrained energy functional (10) yields the following partitioned equation:

$$\begin{bmatrix} \mathbf{K} & \mathbf{C}_{\text{cl}} \\ \mathbf{C}_{\text{cl}}^{\text{T}} & \mathbf{0} \end{bmatrix} \begin{Bmatrix} \mathbf{u} \\ \lambda_{\text{cl}} \end{Bmatrix} = \begin{Bmatrix} \mathbf{f} \\ \mathbf{0} \end{Bmatrix} \tag{11}$$

Note that the physical reaction force vector is given by

$$\mathbf{f}_\lambda = \mathbf{C}_{\text{cl}}\lambda_{\text{cl}} = \begin{bmatrix} 1 & 0 & 0 \\ -1 & 1 & 0 \\ 0 & -1 & 1 \\ 0 & 0 & -1 \end{bmatrix} \begin{Bmatrix} \lambda_{12} \\ \lambda_{23} \\ \lambda_{34} \end{Bmatrix} = \begin{Bmatrix} \lambda_{12} \\ -\lambda_{12} + \lambda_{23} \\ -\lambda_{23} + \lambda_{34} \\ -\lambda_{34} \end{Bmatrix} \tag{12}$$

If one chooses Option 2 as shown in Fig. 2c, the reaction force vector is given by

$$\mathbf{f}_\lambda = \begin{bmatrix} 0 & 0 & -1 \\ 1 & 0 & 0 \\ -1 & 1 & 0 \\ 0 & -1 & 1 \end{bmatrix} \begin{Bmatrix} \bar{\lambda}_{12} \\ \bar{\lambda}_{23} \\ \bar{\lambda}_{41} \end{Bmatrix} = \begin{Bmatrix} -\bar{\lambda}_{41} \\ \bar{\lambda}_{12} \\ -\bar{\lambda}_{12} + \bar{\lambda}_{23} \\ -\bar{\lambda}_{23} + \bar{\lambda}_{41} \end{Bmatrix} \tag{13}$$

Observe that, while the reaction force $\mathbf{f}_\lambda$ is unique, its representation depends on the choice of the constraints with different Lagrange multipliers and with differing computational consequences. Specifically, information flow from one spring to adjacent ones becomes non-uniform when the classical λ-method is used with a set of rank-sufficient constraints. For example, constraint $c_{13} = u_1 - u_3 = 0$ is not explicitly enforced in Option 1 whereas constraint $c_{12} = u_1 - u_2 = 0$ is not explicitly enforced in Option 2. This may delay information flow during iterative solution or design iterations. This is critical in an iterative solution of the governing equations or optimization iterations.

In other words, when Option 1 is adopted as shown in Fig. 2b, there is no intrinsic constraint acting between springs 3 and 4. This means that, if a solution perturbation or design modification is introduced at spring 1, spring 4 will not feel it until at least after third design iterations. Similarly, when Option 2 is adopted as shown in Fig. 2c,

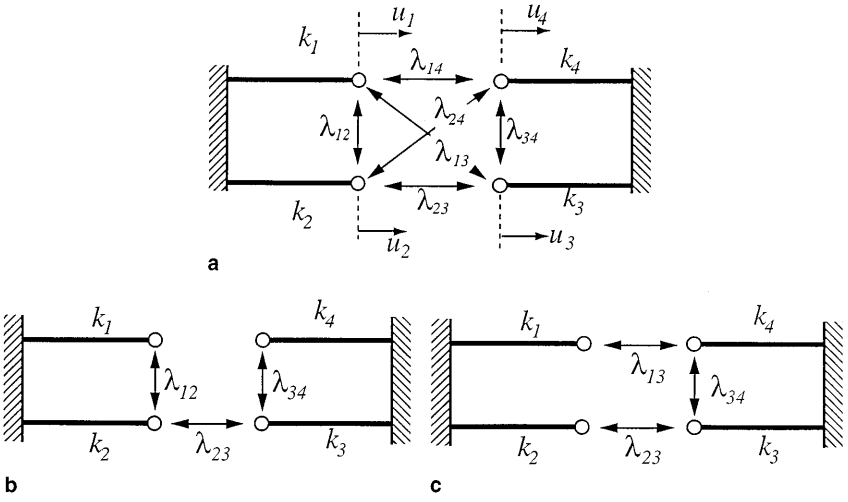

Fig. 2 a–c. Interface constraints by the classical λ-method for 4-spring problem. **a** Fully redundant case; **b** Option 1 of rank-sufficient case; **c** Option 2 of rank-sufficient case

there is no intrinsic constraint acting between springs 1 and 2.

Remark 2.6: One way to achieve an instant information flow from one node to the rest of the partitioned nodes is to invoke the fully redundant constraints as shown in Fig. 2a. This means there have to be 45 classical Lagrange multipliers for 10-node constraints. This not only leads to rank deficiency, but also to increased Lagrange multipliers. Finally, as discussed in Sect. 4, there does not appear to be a rational regularization in conjunction with the classical λ-method when it is used to model interfaces whose surface rigidities are radically different such as metal interacting with rubber-like materials.

2.3
Loss of $(\mathbf{u}, \lambda_{\mathrm{cl}})$-duality for inverse problems

In many structural inverse problems for identifying parameters that are difficult to model or structural damage detection, measured data are often characterized in terms of flexibility instead of stiffness (cf., Park et al., 1998). A structural inverse problem is formulated by partitioning the structure into several substructures and is used to identify substructural parameters. Here, one-to-one duality between the substructural displacements and the Lagrange multipliers for the same substructure plays a crucial role for identification process.

Specifically, consider Fig. 3 where 9 plate elements are partitioned and the flexibility of element (e) is to be identified. First, there are numerous ways of introducing a rank-sufficient set of Lagrange multipliers. For the choice indicated in Fig. 3, the pairing of the substructural displacements and the associated Lagrange multipliers is also given in Fig. 3. Note that they do not form a duality, meaning that there are 4 nodal displacements whereas there are a total of 8 Lagrange multipliers. Of course, one can deliberately choose a set of Lagrange multipliers for element (e) so that $(\mathbf{u}^{(e)}, \lambda_{\mathrm{cl}}^{(e)})$ form their duality. However, this can only be accomplished by affecting non-dualities for other elements.

For more complex problems, a selection of linearly independent set of Lagrange multipliers constitutes essentially the same task that the classical force method has been facing as discussed in Remark 2.6.

3
A localized version of the method of Lagrange multipliers

In this section we first introduce the basic concept of a localized version of the method of Lagrange multipliers, which will be designated subsequently as the localized λ-method. We then show that the localized λ-method leads to a rank-sufficient unique set of constraints regardless of the number of nodes constrained to a node. We then

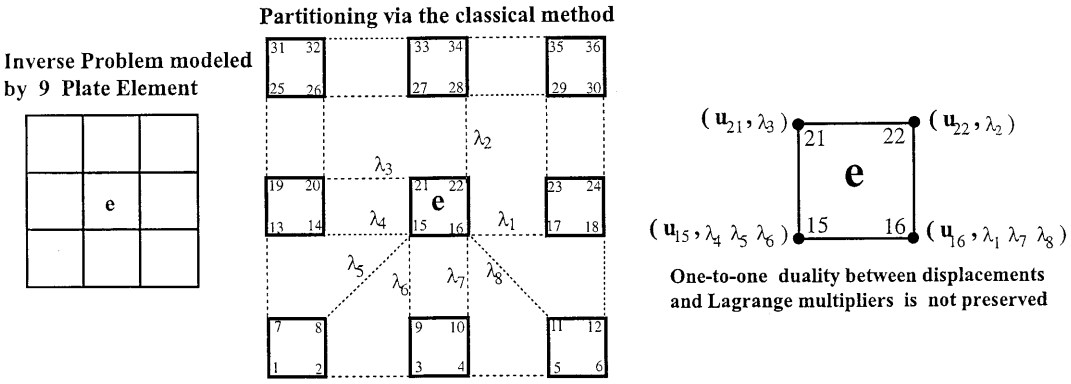

Fig. 3. Inverse problem modeling by the classical λ-method for 9-element plate problem

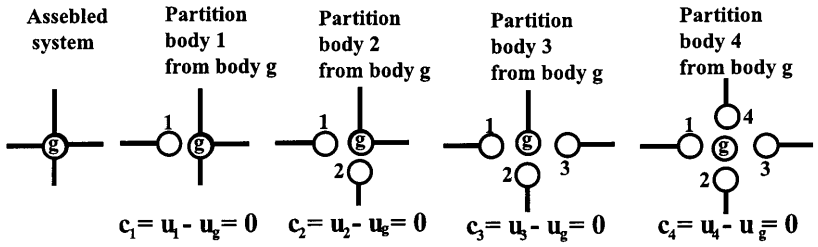

Fig. 4. The multiplier-localization approach to linearly independent constraints

introduce a flexibility normalization procedure that offers an improved modeling of contact, coupled-field problems and parallel transient analysis.

3.1 Basic concept of localized Lagrange multipliers

One thought that came to the present authors' mind to bypass the non-uniqueness of the interface compatibility matrix $\mathbf{C}_{\text{cl}}$ was to employ the following approach.

Let us revisit the problem of partitioning of four bodies discussed in Sect. 2.1. First, we introduce a reference node herein designated g, to which all of the partitioned nodes are constrained. Partitioning body 1 from the reference body g, as illustrated in Fig. 4, gives rise to one constraint:

$$c_1 = \mathbf{u}_1 - \mathbf{u}_g = 0 \tag{14}$$

Second, partitioning body 2 from the reference body g yields:

$$c_2 = \mathbf{u}_2 - \mathbf{u}_g = 0 \tag{15}$$

Third, partitioning body 3 from the reference body g yields:

$$c_3 = \mathbf{u}_3 - \mathbf{u}_g = 0 \tag{16}$$

Finally, partitioning body 4 from the reference body g yields:

$$c_4 = \mathbf{u}_4 - \mathbf{u}_g = 0 \tag{17}$$

The preceding successive four partitioning steps are illustrated in Fig. 4. Note that the constraint relations are characterized by c_i with a single subscript in contrast to the classical λ-method for which c_{ij} is characterized by double subscripts. In other words, the constraints are localized. The method of Lagrange multipliers that adopts the above constraints will be designated as the method of localized Lagrange multipliers or simply the localized λ-method.

Remark 3.1: Observe that the order of partitioning does not affect the resulting constraint conditions. For example, if body 2 is partitioned from the reference body g first, it still gives rise to the same constraint condition, viz., (15) without affecting the rest three constraints. This is in contrast to the dependency of constraints on the order of partitioning discussed in Remark 2.1 using the classical method of Lagrange multipliers.

The constraints given in (14)–(17) lead to the following constraint functional

$$\pi_\ell(\mathbf{u}, \lambda_\ell, \mathbf{u}_g) = \sum_{i=1}^{m} c_i \ \lambda_i \tag{18}$$

where subscript (ℓ) refers to the localized method of Lagrange multipliers, and $m = 4$ is the number of interface nodes constrained at a same node.

The total energy functional of the system is given by augmenting the constraint functional (18) to the virtual work:

$$\begin{aligned}\Pi(\mathbf{u}, \lambda_{\text{cl}}) &= W(\mathbf{u}) + \pi_\ell(\mathbf{u}, \lambda_\ell, \mathbf{u}_g) \\ &= \sum_{i=1}^{N_s} W_i(\mathbf{u}_i) + \sum_{i=1}^{m} c_i \ \lambda_i \end{aligned} \tag{19}$$

The foregoing multiplier localization technique may not be applicable to all possible constraint combinations. It works effectively, however, for a wide spectrum of problems in partitioned analysis wherein constraints $c_i = 0$ consist of linear functions of the partitioned variables. When applicable, its key advantage is that it eliminates concerns about constraint dependencies. Because all bodies are treated equally the computer implementation is simplified. On the minus side it introduces further unknowns, namely the degrees of freedom of the reference body, u_g, in Fig. 4. This is compensated by the reduction of Lagrange multipliers if the number of interacting bodies exceeds 3. For example, if 8 bodies interact, the number of possible multipliers is cut from 28 to 8. For two-body interactions the number of unknowns using the multiplier localization technique becomes twice of those needed by the classical λ-method.

3.2 Equilibrium equations rendered by the localized λ-method

The total energy of the partitioned system for the four-spring system shown in Fig. 5 in terms of the localized Lagrange multiplier λ_ℓ can be expressed:

$$\Pi(\mathbf{u}, \lambda_\ell, \mathbf{u}_g) = \mathbf{u}^{\text{T}} \ (\tfrac{1}{2} \mathbf{K} \ \mathbf{u} - \mathbf{f}) + \lambda_\ell^{\text{T}} \ \mathbf{B}(\mathbf{u} - \mathbf{L}\mathbf{u}_g)$$

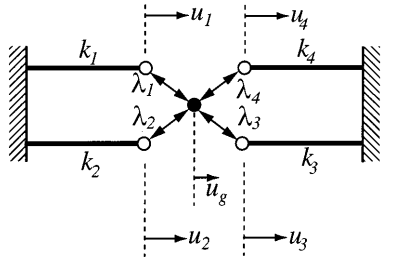

Fig. 5. Four-spring interface modeling by the localized λ-method

$$\mathbf{u} = \begin{Bmatrix} u_1 \\ u_2 \\ u_3 \\ u_4 \end{Bmatrix}, \quad \lambda_\ell = \begin{Bmatrix} \lambda_1 \\ \lambda_2 \\ \lambda_3 \\ \lambda_4 \end{Bmatrix}, \quad \mathbf{f} = 0.25 \begin{Bmatrix} f_1 \\ f_2 \\ f_3 \\ f_4 \end{Bmatrix} \tag{20}$$

$$\mathbf{B}^{\mathrm{T}} = \mathbf{I}(4 \times 4), \quad \mathbf{L}^{\mathrm{T}} = [1 \quad 1 \quad 1 \quad 1]$$

The stationarity of (20) yields the following equilibrium equation:

$$\begin{bmatrix} \mathbf{K} & \mathbf{B} & 0 \\ \mathbf{B}^{\mathrm{T}} & \mathbf{0} & -\mathbf{L}_b \\ 0 & -\mathbf{L}_b^{\mathrm{T}} & 0 \end{bmatrix} \begin{Bmatrix} \mathbf{u} \\ \lambda_\ell \\ \mathbf{u}_g \end{Bmatrix} = \begin{Bmatrix} \mathbf{f} \\ \mathbf{0} \\ \mathbf{0} \end{Bmatrix}, \quad \mathbf{L}_b = \mathbf{B}^{\mathrm{T}}\mathbf{L} \tag{21}$$

Remark 3.2: The above partitioned equation yielded by the localized λ-method consists of three variables $(\mathbf{u}, \lambda_\ell, \mathbf{u}_g)$. Comparing this with that rendered by the classical λ-method (11), we find one distinct feature: the last row of (21), namely, $\mathbf{L}_b^{\mathrm{T}}\ \lambda_\ell = 0$ explicitly enforces Newton's 3rd law at the partitioned interface regardless of the number of nodes constrained.

Remark 3.3: Since every interface node is connected to all its adjacent nodes through the reference node g as can be seen in Fig. 5, each of the reaction forces is transmitted instantly. In addition, the present localized Lagrange multipliers are in fact the physical interface forces at the interface nodes.

Remark 3.4: Figure 6 shows the one-to-one duality between the partitioned substructural boundary displacements and the present localized Lagrange multipliers. This duality plays a pivotal role in inverse problems as well as leading to a direct flexibility equation (Felippa and Park, 1997) that requires no search for selecting a linearly independent set of Lagrange multipliers.

4
Flexibility normalization through the localized λ-method

Consider two springs whose magnitude ratio is either $k_1/k_2 \gg 1$ or $k_1/k_2 \ll 1$ as shown in Fig. 7. When the two springs are partitioned for partitioned analysis or when the two springs are in contact for contact/impact simulation, the constraint functional to enforce the kinematic constraint by the classical λ-method is given by

$$\pi_{\text{classical}}(\mathbf{u}, \lambda_{\text{cl}}) = \lambda_{12}(u_1 - u_2) \tag{22}$$

When using the localized λ-method, the system constraint functional can be normalized as

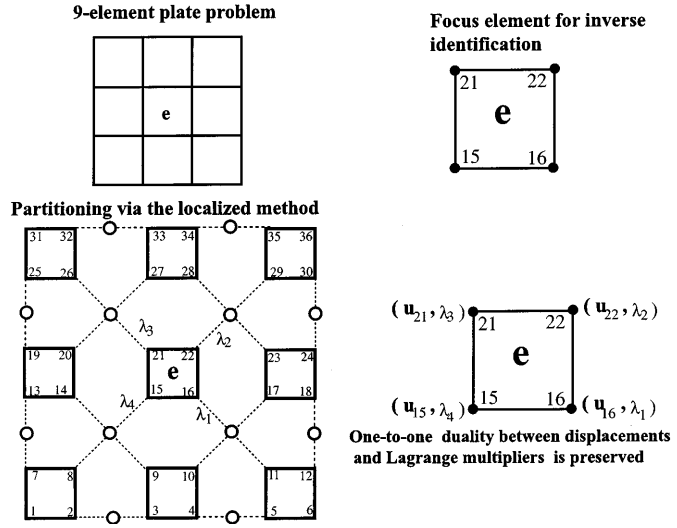

Fig. 6. One-to-one $(\mathbf{u}, \lambda_\ell)$-duality at partition interfaces by the localized λ-method

$$\begin{aligned} \pi_{\text{localized}}(\mathbf{u}, \lambda_\ell, \mathbf{u}_g) &= \lambda_1(u_1 - u_g) + \lambda_2(u_2 - u_g) \\ &= \bar{\lambda}_1 D_1(u_1 - u_g) + \bar{\lambda}_2 D_2(u_2 - u_g) \end{aligned} \tag{23}$$

where D_1 and D_2 are flexibility normalization factors to be determined subsequently.

Observe that by taking appropriate values of D_1 and D_2 for the example case, one effectively scales the unknown Lagrange multipliers λ_1 and λ_2. However, no such scaling possibility exists when using the classical λ-method since each of the Lagrange multipliers enforces two contacting or partitioned nodal displacements to be the same.

In order to determine the flexibility normalization factors, we recall the normalized kinematic constraints and Newton's 3rd law from (23):

$$\begin{aligned} D_1(u_1 - u_g) &= 0 \\ D_2(u_2 - u_g) &= 0 \\ \lambda_1 D_1 + \lambda_2 D_2 &= 0 \end{aligned} \tag{24}$$

where the superscript $\bar{()}$ is dropped for simplicity.

Thus, one finds the least-square solution of the reference nodal displacement u_g as

$$u_g = \frac{D_1^2\ u_1 + D_2^2\ u_2}{D_1^2 + D_2^2} \quad \Rightarrow \quad \dot{u}_g = \frac{D_1^2\ \dot{u}_1 + D_2^2\ \dot{u}_2}{D_1^2 + D_2^2} \tag{25}$$

By invoking the contact enforcement condition of the elementary impact theory, if the impact is to be conservative for two rigid bodies, we must have

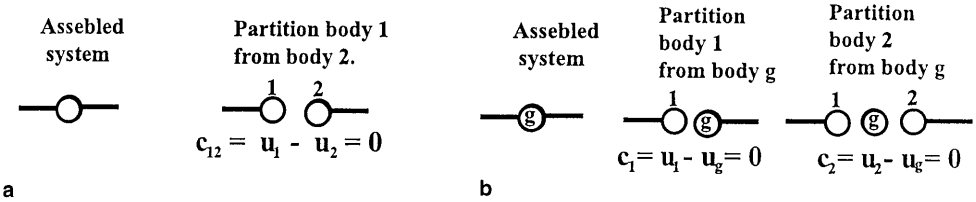

Fig. 7 a, b. Classical and localized λ-methods. **a** Classical method of Lagrange multiplier; **b** a localized of the method of Lagrange multipliers

$$\dot{u}_g = \frac{m_1\ \dot{u}_1 + m_2\ \dot{u}_2}{m_1 + m_2} \quad \Rightarrow \quad D_1^2 = m_1 \quad \text{and} \quad D_2^2 = m_2 \tag{26}$$

Therefore, in order to cover both impact and contact conditions for two elastic bodies, D_1 and D_2 must be, from a dimensional consideration, of the following form:

$$D_1^2 = \frac{m_1}{c\Delta t^2} + k_1, \quad D_2^2 = \frac{m_2}{c\Delta t^2} + k_2 \tag{27}$$

where $\triangle t$ is a characteristic time scale and c is a constant.

Remark 4.1: Note that the preceding relation yields the quasi-static contact with $\triangle t^2 \to \infty$:

$$D_1^2 = k_1, \quad D_2^2 = k_2 \tag{28}$$

Using this relation, the incremental displacement for each body to satisfy the quasi-static contact condition becomes

$$\begin{aligned} \triangle u_1 &= u_1 - u_g = \frac{k_2(u_1 - u_2)}{k_1 + k_2} \\ \triangle u_2 &= u_2 - u_g = \frac{-k_1(u_1 - u_2)}{k_1 + k_2} \end{aligned} \tag{29}$$

which can be used for estimating the contact boundary in an iterative computation of contact problems. For a general dynamic contact problem, k_1 and k_2 should be replaced by D_1^2 and D_2^2 (27), respectively.

Remark 4.2: In addition, the use of the flexibility normalization (23) with the choice of (27) is shown to accelerate the iterative solution of partitioned dynamic equations of motion (cf. Sect. 7).

Remark 4.3: In general a typical substructure contains a large set of interior nodes such that its stiffness may be expressed as

$$\mathbf{K}^{(s)} = \begin{bmatrix} \mathbf{K}_{bb} & \mathbf{K}_{bi} \\ \mathbf{K}_{ib} & \mathbf{K}_{ii} \end{bmatrix}$$

Hence, the Guyan reduced boundary stiffness becomes $\mathbf{K}_{bb}^{(s)} = \mathbf{K}_{bb} - \mathbf{K}_{bi}\ \mathbf{K}_{ii}^{-1}\ \mathbf{K}_{ib}$. Ideally, it would be preferable to use its diagonal. However, since it is usually never formed explicitly in actually computations, it may be practical to use the diagonal of $\mathbf{K}_{bb}$ instead.

Remark 4.4: Finally, the term *flexibility normalization factors* has been adopted from the following observation. Recalling the four-spring example problem considered in Sects. 2 and 3, we have

$$\begin{aligned} \pi_{\text{localized}}(\mathbf{u}, \lambda_\ell, \mathbf{u}_g) = {} & \lambda_1 D_1(u_1 - u_g) + \lambda_2 D_2(u_2 - u_g) \\ & + \lambda_3 D_1(u_3 - u_g) + \lambda_4 D_4(u_4 - u_g) \end{aligned} \tag{30}$$

When this is incorporated, (21) becomes

$$\begin{bmatrix} \mathbf{K} & \mathbf{D}\ \mathbf{B} & \mathbf{0} \\ \mathbf{B}^{\mathrm{T}}\mathbf{D} & \mathbf{0} & -\mathbf{D}\mathbf{L}_b \\ \mathbf{0} & -\mathbf{L}_b^{\mathrm{T}}\mathbf{D} & \mathbf{0} \end{bmatrix} \begin{Bmatrix} \mathbf{u} \\ \lambda_\ell \\ \mathbf{u}_g \end{Bmatrix} = \begin{Bmatrix} \mathbf{f} \\ \mathbf{0} \\ \mathbf{0} \end{Bmatrix}, \tag{31}$$

$\mathbf{D}_{ii} = \sqrt{k_i}$

Solving for $\mathbf{u}$ and substituting into the second equation of (31) we obtain

$$\begin{bmatrix} \mathbf{B}^{\mathrm{T}}\mathbf{D}\ \mathbf{K}^{-1}\ \mathbf{D}\ \mathbf{B} & \mathbf{D}\ \mathbf{L}_b \\ \mathbf{L}_b^{\mathrm{T}}\mathbf{D} & 0 \end{bmatrix} \begin{Bmatrix} \lambda_\ell \\ \mathbf{u}_g \end{Bmatrix} = \begin{Bmatrix} \mathbf{B}^{\mathrm{T}}\mathbf{D}\mathbf{K}^{-1}\mathbf{f} \\ \mathbf{0} \end{Bmatrix},$$

$$\mathbf{D} = \begin{bmatrix} \sqrt{k_1} & 0 & 0 & 0 \\ 0 & \sqrt{k_2} & 0 & 0 \\ 0 & 0 & \sqrt{k_3} & 0 \\ 0 & 0 & 0 & \sqrt{k_4} \end{bmatrix}$$

$$\mathbf{F}_b = \mathbf{B}^{\mathrm{T}}\mathbf{D}\ \mathbf{K}^{-1}\ \mathbf{D}\ \mathbf{B} = \mathbf{I}, \tag{32}$$

$$\mathbf{K}^{-1} = \begin{bmatrix} {k_1}^{-1} & 0 & 0 & 0 \\ 0 & {k_2}^{-1} & 0 & 0 \\ 0 & 0 & {k_3}^{-1} & 0 \\ 0 & 0 & 0 & {k_4}^{-1} \end{bmatrix}$$

Observe that $\mathbf{D}$ has the effect of normalizing the flexibility matrix $\mathbf{F}_b$. Of course, for multidimensional problems $\mathbf{F}_b$ does in no way become an identity matrix as only $\mathbf{D}$ is diagonal. However, it offers a surprisingly beneficial impact on the computational efficiency as discussed in Sect. 7 on numerical examples.

5 Comparison of the localized and classical λ-methods

As a basis of comparing the classical λ-method with the present localized λ-method, we recall from (31) that the partitioned equilibrium equation given by the localized λ-method consists of three variables $(\mathbf{u}, \lambda_\ell, \mathbf{u}_g)$. Observe that $\mathbf{u}_g$ can be projected out from (31) by pre and post-multiplying the second row and second column, respectively, by

$$\mathbf{P}_D = \mathbf{I} - \mathbf{D}\mathbf{L}_b\ (\mathbf{L}_b^{\mathrm{T}}\mathbf{D}^2\mathbf{L}_b)^{-1}\ \mathbf{L}_b^{\mathrm{T}}\mathbf{D} \tag{33}$$

to yield:

$$\begin{bmatrix} \mathbf{K} & \mathbf{D}\ \mathbf{P}_D\ \mathbf{B} \\ \mathbf{B}^{\mathrm{T}}\mathbf{D}\ \mathbf{P}_D & \mathbf{0} \end{bmatrix} \begin{Bmatrix} \mathbf{u} \\ \bar{\lambda}_\ell \end{Bmatrix} = \begin{Bmatrix} \mathbf{f} \\ \mathbf{0} \end{Bmatrix} \tag{34}$$

In particular, when no flexibility normalization is employed in conjunction with the localized λ-method, i.e., $\mathbf{D} = \mathbf{I}$, the preceding equation reduces to

$$\begin{bmatrix} \mathbf{K} & \mathbf{P}_L \\ \mathbf{P}_L & \mathbf{0} \end{bmatrix} \begin{Bmatrix} \mathbf{u} \\ \bar{\lambda}_\ell \end{Bmatrix} = \begin{Bmatrix} \mathbf{f} \\ \mathbf{0} \end{Bmatrix}, \quad \text{with} \quad \mathbf{D} = \mathbf{I} \quad \text{since} \quad \mathbf{P}_L = \mathbf{I} - \mathbf{L}_b(\mathbf{L}_b^{\mathrm{T}}\ \mathbf{L}_b)^{-1}\ \mathbf{L}_b \tag{35}$$

It can be shown that the projection operator $\mathbf{P}_L$ has the following specific forms for 2, 3 and 4-node interfaces, respectively:

$$\mathbf{P}_L = \frac{1}{2}\begin{bmatrix} 1 & -1 \\ -1 & 1 \end{bmatrix} = \frac{1}{2}\begin{bmatrix} 1 \\ -1 \end{bmatrix} \cdot \begin{bmatrix} 1 & 1 \end{bmatrix}$$

$$\mathbf{P}_L = \frac{1}{3}\begin{bmatrix} 2 & -1 & -1 \\ -1 & 2 & -1 \\ -1 & -1 & 2 \end{bmatrix}$$

$$= \frac{1}{3}\begin{bmatrix} 1 & 1 & 0 \\ -1 & 0 & 1 \\ 0 & -1 & -1 \end{bmatrix} \cdot \begin{bmatrix} 1 & -1 & 0 \\ 1 & 0 & -1 \\ 0 & 1 & -1 \end{bmatrix}$$

$$\mathbf{P}_L = \frac{1}{4}\begin{bmatrix} 3 & -1 & -1 & -1 \\ -1 & 3 & -1 & -1 \\ -1 & -1 & 3 & -1 \\ -1 & -1 & -1 & 3 \end{bmatrix}$$

$$= \frac{1}{4}\begin{bmatrix} 1 & 1 & 1 & 0 & 0 & 0 \\ -1 & 0 & 0 & 1 & 1 & 0 \\ 0 & -1 & 0 & -1 & 0 & 1 \\ 0 & 0 & -1 & 0 & -1 & -1 \end{bmatrix} \cdot \begin{bmatrix} 1 & -1 & 0 & 0 \\ 1 & 0 & -1 & 0 \\ 1 & 0 & 0 & -1 \\ 0 & 1 & -1 & 0 \\ 0 & 1 & 0 & -1 \\ 0 & 0 & 1 & -1 \end{bmatrix} \tag{36}$$

$$\Downarrow$$

$$\mathbf{P}_L = \frac{1}{\sqrt{m}}\mathbf{C}_{\text{cl}}\ (m) \cdot \frac{1}{\sqrt{m}}\mathbf{C}_{\text{cl}}\ (m)^{\text{T}}$$

where m is the number of interfaces and $\mathbf{C}_{\text{cl}}(m)$ is the fully redundant constraint conditions. For example, for an interface involving 8 nodes the size of $\mathbf{C}_{\text{cl}}(m)$ is (28×8), implying that the number of Lagrange multipliers necessary for the optimum constraints have to be 28.

The foregoing analysis suggests the following:

1. Comparing (35) with the partitioned equation (11) rendered by the classical λ-method, we conclude that the constraint operator $\mathbf{C}_{\text{cl}}\ (m)$ utilizes only one part of $\mathbf{P}_L$ as can be seen from (36). Observe that $\mathbf{P}_\ell$ explicitly satisfies Newton's 3rd law given by the third row of (31), namely, $\mathbf{L}_b^{\text{T}}\lambda_\ell = 0$. On the other hand, the partitioned equation (11) rendered by the classical λ-method satisfies Newton's 3rd law only after the partitioned displacement $\mathbf{u}$ has converged to a correct solution.
2. As for a similar flexibility normalization for the partitioned equation rendered by the classical λ-method, one is tempted to modify $\mathbf{C}_{\text{cl}}\ (m)$ by

$$\mathbf{C}_{\text{cl}}^{\text{T}}\ (m) \quad \Rightarrow \quad \mathbf{D}_{\text{cl}}\ \mathbf{C}_{\text{cl}}^{\text{T}}\ (m) \tag{37}$$

To the best of our ability, there does not appear to be an equivalent form from the preceding modification to the present projector $\mathbf{P}_D$ given in (33).

6 Application: solution of partitioned quasi-static flexibility equation

One popular application of the method of Lagrange multipliers has been for parallel iterative solution of the partitioned flexibility equation for structural systems. The other is the enforcement of contact conditions. In terms of both the classical and present localized λ-methods, the iterative solution of the partitioned equilibrium equations and the contact enforcement of substructural systems constitute the same problem. To this end, we first present the partitioned equations of motion employing the present localized λ-method (Felippa and Park, 1997; Park and Felippa, 1998a) which reduce to partitioned flexibility equations upon eliminating the partitioned displacements. The flexibility normalization is then introduced to both dynamic and quasi-static partitioned flexibility equations. The performance of these flexibility equations are then assessed in Sect. 7.

6.1 Partitioned quasi-static flexibility equations

Now consider for example assembled continuum structure partitioned into individual elements as shown in Fig. 8. The individual nodal displacements $\mathbf{u}$ are related to the assembled global displacements $\mathbf{u}_g$ through the assembly matrix $\mathbf{L}$ according to:

$$\mathbf{u} - \mathbf{L}\ \mathbf{u}_g = 0 \tag{38}$$

Hence, the discrete energy functional can be expressed in terms of the partitioned elemental displacements as

$$\Pi(\mathbf{u}_g, \lambda, \mathbf{u}) = \mathbf{u}^{\text{T}}\ (\tfrac{1}{2}\ \mathbf{K}\ \mathbf{u} - \mathbf{f}) + \lambda_\ell^{\text{T}}\mathbf{B}^{\text{T}}\ (\mathbf{u} - \mathbf{L}\ \mathbf{u}_g) \tag{39}$$

where λ_ℓ are the Lagrange multipliers that enforce the partition boundary kinematical compatibility condition (38), $\mathbf{B}$ is a Boolean matrix that extracts the partition boundary degrees of freedom, and $\mathbf{f}$ is the applied force.

For computational considerations, it is convenient to decompose the substructural displacement $\mathbf{u}$ according to (Park and Felippa, 1998a):

$$\mathbf{u} = \mathbf{d} + \mathbf{R}\boldsymbol{\alpha} \tag{40}$$

where $\mathbf{R}$ are the rigid-body modes, and $\mathbf{d}$ and $\boldsymbol{\alpha}$ are the generalized displacements corresponding to the deformation and rigid-body motions, respectively.

Substituting this into (39) and carrying out its variation for its stationarity yields the following discrete equation:

$$\begin{bmatrix} \mathbf{K} & -\mathbf{B} & \mathbf{0} & \mathbf{0} \\ -\mathbf{B}^{\text{T}} & \mathbf{0} & -\mathbf{R}_b & \mathbf{L}_b \\ \mathbf{0} & -\mathbf{R}_b^{\text{T}} & \mathbf{0} & \mathbf{0} \\ \mathbf{0} & \mathbf{L}_b^{\text{T}} & \mathbf{0} & \mathbf{0} \end{bmatrix} \begin{Bmatrix} \mathbf{d} \\ \alpha_\ell \\ \alpha_r \\ \mathbf{u}_{gb} \end{Bmatrix} = \begin{Bmatrix} \mathbf{f} \\ 0 \\ -\mathbf{R}^{\text{T}}\mathbf{f} \\ 0 \end{Bmatrix} \tag{41}$$

$$\mathbf{R}_b = \mathbf{B}^{\text{T}}\mathbf{R}, \quad \mathbf{L}_b = \mathbf{B}^{\text{T}}\mathbf{L}$$

Elimination of the deformation variable $\mathbf{d}$ leads to the following quasi-static partitioned flexibility equation:

$$\begin{bmatrix} \mathbf{B}^{\text{T}}\mathbf{K}^{+}\mathbf{B} & -\mathbf{R}_b & \mathbf{L}_b \\ -\mathbf{R}_b^{\text{T}} & \mathbf{0} & \mathbf{0} \\ \mathbf{L}_b^{\text{T}} & \mathbf{0} & \mathbf{0} \end{bmatrix} \begin{Bmatrix} \lambda_\ell \\ \boldsymbol{\alpha} \\ \mathbf{u}_{gb} \end{Bmatrix} = \begin{Bmatrix} \mathbf{B}^{\text{T}}\ \mathbf{K}^{+}\mathbf{f} \\ -\mathbf{R}^{\text{T}}\mathbf{f} \\ 0 \end{Bmatrix}, \tag{42}$$

$$\mathbf{R}_b = \mathbf{B}^{\text{T}}\mathbf{R}$$

$$\mathbf{u} = \mathbf{K}^{+}\ (\mathbf{f} - \mathbf{B}\ \lambda_\ell) + \mathbf{R}\boldsymbol{\alpha}$$

where $\mathbf{K}^{+}$ is a generalized inverse of $\mathbf{K}$.

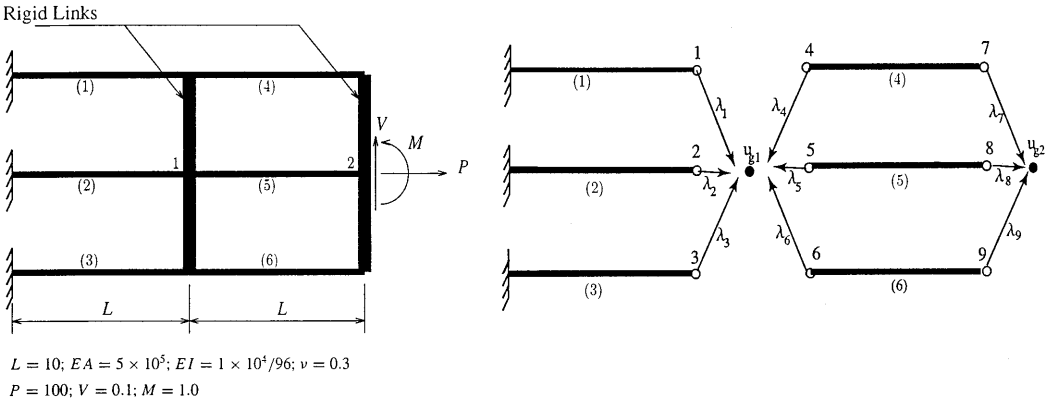

Fig. 8a, b. Three beams rigidly linked at half station and the tip end. **a** Problem to be solved; **b** Lagrange multipliers after partitioning by the localized λ-method

6.2 Normalized partitioned flexibility equations

Following the four-spring example case given by (29) and (30), the static partitioned equations (42) are modified as

$$\begin{bmatrix} \hat{\mathbf{F}}_b & -\mathbf{D}\,\mathbf{R}_b & \mathbf{D}\,\mathbf{L}_b \\ -\mathbf{R}_b^{\mathrm{T}}\,\mathbf{D} & \mathbf{0} & \mathbf{0} \\ \mathbf{L}_b^{\mathrm{T}}\,\mathbf{D} & \mathbf{0} & \mathbf{0} \end{bmatrix} \begin{Bmatrix} \lambda_D \\ \boldsymbol{\alpha} \\ \mathbf{u}_{gb} \end{Bmatrix} = \begin{Bmatrix} \mathbf{D}\,\mathbf{B}^{\mathrm{T}}\,\mathbf{K}^{+}\mathbf{f} \\ -\mathbf{R}^{\mathrm{T}}\mathbf{f} \\ \mathbf{0} \end{Bmatrix}$$

$$\hat{\mathbf{F}}_b = \mathbf{D}\,\mathbf{B}^{\mathrm{T}}\,\mathbf{K}^{+}\,\mathbf{B}\,\mathbf{D} = \mathbf{D}\,\mathbf{F}_b\,\mathbf{D}, \tag{43}$$

$$\mathbf{D} = \sqrt{\mathrm{diag}\ \mathbf{K}_{bb}}, \quad \lambda_D = \mathbf{D}\,\lambda_\ell$$

$$\mathbf{u} = \mathbf{K}^{+}\,(\mathbf{f} - \mathbf{B}\,\mathbf{D}\,\lambda_D) + \mathbf{R}\boldsymbol{\alpha}$$

where $\mathbf{D}$ involves only the partition boundary attributes, and $\mathbf{K}_{bb}$ contains the partition boundary stiffness components.

The preconditioned conjugate gradient solution strategy adopted iterates on the following residual (see, e.g., Justino et al. (1997) for details):

$$\begin{aligned} \mathbf{r}_P &= \mathbf{P}_\ell\,\mathbf{S}^{+}\,\mathbf{P}_\ell\,(\mathbf{g}_\lambda - \hat{\mathbf{F}}_b\,\lambda_\ell), \quad \mathbf{S}^{+} = \hat{\mathbf{F}}_b^{+} \\ \mathbf{P}_\ell &= \mathbf{P}_D - \mathbf{G}_\alpha(\mathbf{G}_\alpha^{\mathrm{T}}\mathbf{G}_\alpha)^{-1}\mathbf{G}_\alpha^{\mathrm{T}} \\ \mathbf{P}_D &= \mathbf{I} - \mathbf{D}\,\mathbf{L}_b(\mathbf{L}_b^{\mathrm{T}}\,\mathbf{D}^2\,\mathbf{L}_b)^{-1}\,\mathbf{L}_b^{\mathrm{T}}\,\mathbf{D} \\ \mathbf{G}_\alpha &= \mathbf{P}_D\,\mathbf{D}\,\mathbf{R}_b, \quad \mathbf{g}_\lambda = \mathbf{B}^{\mathrm{T}}\,\mathbf{D}\,\mathbf{K}^{+}\mathbf{f} \end{aligned} \tag{44}$$

Observe that the case without flexibility normalization is recovered by setting $\mathbf{D} = \mathbf{I}$.

6.3 Comparison with the DFETI-1 algorithm (Farhat and Roux, 1991; Farhat et al., 1994)

Farhat and Roux (1991), Farhat et al. (1994) presented the DFETI-1 method that employs the following preconditioned residual:

$$\begin{aligned} \mathbf{r}_{(\mathrm{FR})} &= \mathbf{P}_{\mathrm{cl}}^{\mathrm{T}}\,\mathbf{F}_{\mathrm{cl}}^{+}\,\mathbf{P}_{\mathrm{cl}}\,(\mathbf{D} - \mathbf{F}_{\mathrm{cl}}\lambda_{\mathrm{cl}}), \\ \mathbf{F}_{\mathrm{cl}} &= \mathbf{C}_{\mathrm{cl}}^{\mathrm{T}}\,\mathbf{K}^{+}\,\mathbf{C}_{\mathrm{cl}}, \\ \mathbf{F}_{\mathrm{cl}}^{+} &= \mathbf{C}_{\mathrm{cl}}^{\mathrm{T}}\,\mathbf{K}_{bb}^{S}\,\mathbf{C}_{\mathrm{cl}}, \\ \mathbf{d} &= \mathbf{C}_{\mathrm{cl}}^{\mathrm{T}}\,\mathbf{K}^{+}\,\mathbf{f}, \end{aligned} \tag{45}$$

$$\mathbf{P}_{\mathrm{cl}} = \mathbf{I} - \mathbf{G}_{\mathrm{cl}}(\mathbf{G}_{\mathrm{cl}}^{\mathrm{T}}\mathbf{G}_{\mathrm{cl}})^{-1}\mathbf{G}_{\mathrm{cl}}^{\mathrm{T}},$$

$$\mathbf{G}_{\mathrm{cl}} = \mathbf{C}_{\mathrm{cl}}\mathbf{R}$$

where $\mathbf{C}_{\mathrm{cl}}^{\mathrm{T}}$ enforces interface displacement constraints via the classical method of Lagrange multipliers, $\mathbf{K}_{bb}^{S}$ is the partition boundary Schur complement of $\mathbf{K}$.

The present static algorithm (44) and the algorithm of Farhat and Roux (45) are comparable in terms of computational effort. However, we observe that the present simple algorithm is fundamentally different from the latter.

First, one may introduce the heterogeneous preconditioner of Rixen and Farhat (1997) in place of $\mathbf{F}_{\mathrm{cl}}^{+}$, which may be symbolically written as

$$\hat{\mathbf{F}}_{\mathrm{cl}}^{+} = \hat{\mathbf{C}}_{\mathrm{cl}}^{\mathrm{T}}\,\mathbf{K}_{bb}^{S}\,\hat{\mathbf{C}}_{\mathrm{cl}} \tag{46}$$

where $\hat{\mathbf{C}}_{\mathrm{cl}}$ for a two-spring interface (see Fig. 3) is given by

$$\hat{\mathbf{C}}_{\mathrm{cl}} = [\,\hat{c}_1 \quad \hat{c}_2\,], \quad c_1 = \frac{k_2}{k_1 + k_2}, \quad c_2 = \frac{k_1}{k_1 + k_2} \tag{47}$$

It can be shown that $\hat{\mathbf{C}}_{\mathrm{cl}}$ used in Rixen and Farhat (1997) can be related to the present flexibility normalized projector $\mathbf{P}_D$ by

$$\mathbf{D}^{-1}\,\mathbf{P}_D\,\mathbf{D} = \mathbf{D}^{-1}\,\mathbf{P}_D^2\,\mathbf{D} = \hat{\mathbf{C}}_{\mathrm{cl}}\,\mathbf{C}_{\mathrm{cl}}^{\mathrm{T}} \tag{48}$$

The preconditioned solution matrices of the two algorithms thus become

$$\begin{aligned} &\text{Present Algorithm:} && \mathbf{P}_\ell\,\hat{\mathbf{F}}_b^{+}\,\mathbf{P}_\ell\,\hat{\mathbf{F}}_b = \mathbf{P}_\ell\,[\mathbf{P}_D\,\mathbf{D}^{-1}\mathbf{F}_b^{-1}\,\mathbf{D}^{-1}\,\mathbf{P}_D]\cdot\mathbf{P}_\ell\cdot[\mathbf{D}\,\mathbf{F}_b\,\mathbf{D}\,] \\ &\text{Rixen/Farhat} && \\ &\text{Preconditioner (1997):} && \mathbf{P}_{\mathrm{cl}}^{\mathrm{T}}\hat{\mathbf{F}}_{\mathrm{cl}}^{+}\,\mathbf{P}_{\mathrm{cl}}\,\mathbf{F}_{\mathrm{cl}} = \mathbf{P}_{\mathrm{cl}}^{\mathrm{T}}\,[\hat{\mathbf{C}}_{\mathrm{cl}}^{\mathrm{T}}\,\mathbf{F}_b^{-1}\,\hat{\mathbf{C}}_{\mathrm{cl}}]\,\mathbf{P}_{\mathrm{cl}}\,[\mathbf{C}_{\mathrm{cl}}^{\mathrm{T}}\,\mathbf{F}_b\,\mathbf{C}_{\mathrm{cl}}] \end{aligned} \tag{49}$$

For the special case when every partition is devoid of floating modes, that is fully constrained, we have from (49):

$$\begin{aligned}
&\text{Present Algorithm:} && \mathbf{P}_\ell\ \hat{\mathbf{F}}_b^{+}\ \mathbf{P}_\ell\ \hat{\mathbf{F}}_b \Rightarrow \mathbf{P}_D\ \mathbf{D}^{-1}[\mathbf{F}_b^{-1}\ \mathbf{D}^{-1}\ \mathbf{P}_D\mathbf{D}\ \mathbf{F}_b]\ \mathbf{D}\\
&\text{Rixen/Farhat} && \mathbf{P}_{\mathrm{cl}}^{\mathrm{T}}\hat{\mathbf{F}}_{\mathrm{cl}}^{+}\ \mathbf{P}_{\mathrm{cl}}\ \mathbf{F}_{\mathrm{cl}} \Rightarrow \hat{\mathbf{C}}_{\mathrm{cl}}^{\mathrm{T}}\ [\mathbf{F}_b^{-1}\ \hat{\mathbf{C}}_{\mathrm{cl}}\mathbf{C}_{\mathrm{cl}}^{\mathrm{T}}\ \mathbf{F}_b]\ \mathbf{C}_{\mathrm{cl}}\\
&\text{Preconditioner (1997):} && \quad = \hat{\mathbf{C}}_{\mathrm{cl}}^{\mathrm{T}}\ [\mathbf{F}_b^{-1}\ \mathbf{D}^{-1}\ \mathbf{P}_D\mathbf{D}\ \mathbf{F}_b]\ \ \mathbf{C}_{\mathrm{cl}}
\end{aligned} \tag{50}$$

Hence, the convergence rate of the two methods will be the same for partitions without any floating modes. In other words, the Rixen and Farhat preconditioner $\hat{\mathbf{F}}_{\mathrm{cl}}^{+}$ and the present normalized preconditioner $\hat{\mathbf{F}}_b^{+}$ are algorithmically equivalent.

For a general case of partitions having rigid body modes, however, the two algorithms are different due to their fundamental difference in the projectors, $\mathbf{P}_\ell$ and $\mathbf{P}_{\mathrm{cl}}$. Specifically, the difference can be observed by comparing the two projectors:

$$\begin{aligned}
&\text{Present Normalized Projector:} && \mathbf{P}_\ell = \mathbf{P}_D - \mathbf{P}_D\ \mathbf{D}\ \mathbf{R}_b(\mathbf{R}_b^{\mathrm{T}}\ \mathbf{D}\mathbf{P}_D\ \mathbf{D}\ \mathbf{R}_b)^{-1}\mathbf{R}_b^{\mathrm{T}}\ \mathbf{D}\ \mathbf{P}_D\\
&&& \mathbf{P}_D = \mathbf{I} - \mathbf{D}\ \mathbf{L}_b(\mathbf{L}_b^{\mathrm{T}}\ \mathbf{D}^2\ \mathbf{L}_b)^{-1}\ \mathbf{L}_b^{\mathrm{T}}\ \mathbf{D}\\
&\text{DFETI-1 projector:} && \mathbf{P}_{\mathrm{cl}} = \mathbf{P}_{\mathrm{cl}} = \mathbf{I} - \mathbf{G}_{\mathrm{cl}}(\mathbf{G}_{\mathrm{cl}}^{\mathrm{T}}\mathbf{G}_{\mathrm{cl}})^{-1}\mathbf{G}_{\mathrm{cl}}^{\mathrm{T}},\quad \mathbf{G}_{\mathrm{cl}} = \mathbf{C}_{\mathrm{cl}}\mathbf{R}
\end{aligned} \tag{51}$$

Observe that the present projector $\mathbf{P}_\ell$ incorporates the flexibility normalization effect whereas that of the DFETI-1 is independent of the heterogeneous preconditioning operator $\hat{\mathbf{C}}_{\mathrm{cl}}$. Since the computational overheads per iteration of the present algorithm (44) and the DFETI-1 algorithm (45) are equivalent, it would be interesting to see if the present flexibility-normalized projector would offer any iteration advantage.

For comparison purposes Table 1 list the five algorithms classified according to their preconditioner and projector (or coarse solver).

7 Illustrative problems

Four example problems are used to illustrate the performance of the present localized λ-method. The first is a comparison of the computational efficiency of the partitioned flexibility equations employing the present flexibility-normalized, localized λ-method with that of employing the classical λ-method. The second is a plane stress problem consisting of four subdomains with two heterogeneous materials. The third is a beam tower that gives rise to geometrical heterogeneities as the axial (membrane) forces interact with the bending forces even though every member of the tower beam elements has the same cross section and material properties. Finally, the fourth problem illustrates the performance of a simple partitioned dynamic algorithm to assess the applicability of the flexibility normalization for dynamic contact enforcement as well as parallel iterative solution.

7.1 Importance of redundancies in the classical λ-method

Let us consider the problem shown in Fig. 8a. When the structure is partitioned into six beam elements, the localized λ-method gives rise to six and three Lagrange multipliers at the mid and tip-end nodes, respectively, as shown in Fig. 8b. On the other hand, Fig. 9 illustrates a rank-sufficient and fully redundant modeling of the interfaces by the classical λ-method.

Figure 10 shows the global residual vs. the iteration number for four different modeling of the interface constraints. The measure of solution error at each iteration stage is given by

Table 1. Classification of five static algorithm compared

	DFETI-1	DFETI-1P	AFETI-1	AFETI-1PC	AFETI-1P
Preconditioner	$\bar{\mathbf{W}}\mathbf{C}_\lambda^{\mathrm{T}}\mathbf{K}_{bb}^{S}\mathbf{C}_\lambda\bar{\mathbf{W}}$	$\hat{\mathbf{C}}_\lambda^{\mathrm{T}}\mathbf{K}_{bb}^{S}\hat{\mathbf{C}}_\lambda$	$\mathbf{P}_L\mathbf{K}_{bb}^{S}\mathbf{P}_L$	$\mathbf{P}_D\bar{\mathbf{D}}\mathbf{K}_{bb}^{S}\bar{\mathbf{D}}\mathbf{P}_D$	Same as AFETI-1PC
Projector	$\mathbf{P}_{\mathrm{cl}} = \mathbf{I} - \mathbf{G}_{\mathrm{cl}}(\mathbf{G}_{\mathrm{cl}}^{\mathrm{T}}\mathbf{G}_{\mathrm{cl}})^{-1}\mathbf{G}_{\mathrm{cl}}^{\mathrm{T}}$	Same as DFETI-1	$\mathbf{P}_\ell = \mathbf{I} - \mathbf{G}_\ell(\mathbf{G}_\ell^{\mathrm{T}}\mathbf{G}_\ell)^{-1}\mathbf{G}_\ell^{\mathrm{T}}$	$\mathbf{P}_\ell = \mathbf{I} - \mathbf{G}_D(\mathbf{G}_D^{\mathrm{T}}\mathbf{G}_D)^{-1}\mathbf{G}_D^{\mathrm{T}}$	Same as AFETI-1
	$\mathbf{G}_{\mathrm{cl}} = \mathbf{C}_{\mathrm{cl}}\mathbf{R}$		$\mathbf{G}_\ell = \mathbf{P}_L\mathbf{B}^{\mathrm{T}}\mathbf{R}$	$\mathbf{G}_D = \mathbf{P}_D\mathbf{D}\mathbf{B}^{\mathrm{T}}\mathbf{R}$	

Where $\bar{\mathbf{W}} = \mathbf{W}^{-1}$ and $\bar{\mathbf{D}} = \mathbf{D}^{-1}$
Algorithm Designation:
DFETI-1: Method of Farhat and Roux as summarized in (45).
DFETI-1P: Method of Farhat and Roux where the preconditioner is replaced by Rixen and Farhat (1997) as summarized in (47) and (50).
AFETI-1: Method of Park, Justino and Felippa (1997) that can be obtained by setting $\mathbf{D} = \mathbf{I}$ in (44).
AFETI-1PC: Method as summarized in (44).
AFETI-1P: Method of (44) except the projector $\mathbf{P}_\ell$ is specialized by setting $\mathbf{D} = \mathbf{I}$.

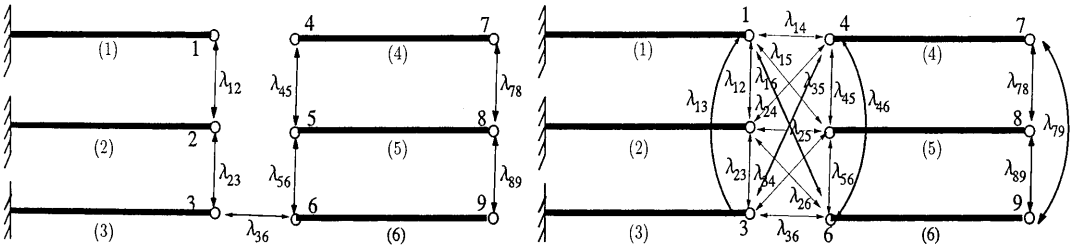

Fig. 9a, b. Modeling of partitioned interface constraints by the classical λ-method. **a** Rank-sufficient case (this is one of many possible choices); **b** redundant but computationally optimal case (There are a total of 15 and 3 multipliers for the two interfaces)

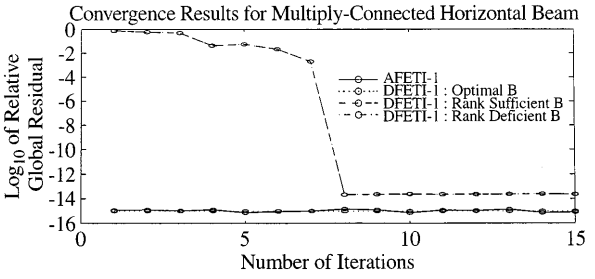

Fig. 10. Global residual vs. iteration number for beam example problem

$$\mathbf{r}_g = |\mathbf{f}_g - \mathbf{K}_g\ \mathbf{u}_g|/|\mathbf{f}_g| \tag{52}$$

The AFETI residual curve is obtained by iterating on the residual vector given by (51), which adopts the Lagrange multipliers shown in Fig. 8b and converges in one iteration.

The residual curves designated as DFETI-1 have been obtained by using the partitioned flexibility equation employing the classical λ-method (Farhat and Roux, 1991; Farhat et al., 1994) as summarized in (44). When one chooses the rank-sufficient Lagrange multipliers as shown in Fig. 9a, 8 iterations are required to obtain a converged solution. Observe that, when the fully redundant Lagrange multipliers are utilized as shown in Fig. 9b, the DFETI-1 method also converges in one iteration. This is because the information flow from one partitioned node to the rest is not instantaneous, whereas for the AFETI-1 method and the DFETI-1 method with fully redundant constraints the information flow is instant.

The DFETI-1 method with various intermediate redundant constraints was also tested. The results indicate that only with the full redundancies of the classical λ-method the DFETI-1 method converges in one iteration. This illustrates that the AFETI-1 algorithm employing the localized λ-method offers the same convergence performance as the fully redundant DFETI-1 method.

7.2 Inverse problem: identification of substructural flexibility

The partitioned quasi-static equation (46) can be used to identify substructural flexibility starting the known global flexibility $\mathbf{F}_g = \mathbf{K}_g$. To this end, solving for $(\lambda_\ell, \boldsymbol{\alpha})$ and substituting them into

$$\mathbf{u} = \mathbf{L}\mathbf{u}_g = \mathbf{L}\mathbf{F}_g\mathbf{f}_g \tag{53}$$

one obtains the following Ricatti-like equation:

$$\mathbf{F} = \mathbf{L}\ \mathbf{F}_g\ \mathbf{L}^{\mathrm{T}} + \ \mathbf{F}\ \{\mathbf{B}\ \mathbf{F}_B^{-1}\ [\mathbf{I} - \mathbf{L}_b\ \mathbf{F}_L\ \mathbf{L}_b^{\mathrm{T}}\ \mathbf{F}_B^{-1}]\ \mathbf{B}^{\mathrm{T}}\ \mathbf{F}\}$$
$$\mathbf{F} = \mathbf{K}^{+}, \quad \mathbf{F}_B = (\mathbf{B}^{\mathrm{T}}\ \mathbf{F}\ \mathbf{B}), \quad \mathbf{F}_L = (\mathbf{L}_b^{\mathrm{T}}\ \mathbf{F}_B^{-1}\ \mathbf{L}_b)^{-1} \tag{54}$$

$\mathbf{F}$ is called the substructural flexibility matrix.

In order to demonstrate the utility of the above equation for identifying the substructural flexibility matrices of block diagonal form, a free-free ladder structure shown in Table 2 is chosen from Park, Reich and Alvin (1997). The ladder is modeled with eight plane beam elements which include axial stiffness. In the present numerical experiment, the global stiffness matrix is generated analytically. The simulated global flexibility matrix is thus $\mathbf{F}_g = \mathbf{K}_g^{-1}$ as the starting point. Using the global flexibility as the known flexibility, the elemental flexibility $\mathbf{F}$ was determined by solving for $\mathbf{F}$ via a homotopy nonlinear iteration method (Richter and Collins, 1989).

Table 2 shows the convergence of the elemental eigenvalues of horizontal mid-element 2 shown in Figure 6. As can be seen in the above table, the initial errors of the two substructural bending eigenvalues are 74% and 6%, respectively. However, after iterations, the extracted substructural flexibility matrix yields the two bending modes with four-digit accuracy.

7.3 Iterative solutions of partitioned quasi-static plane stress problem

Figure 11 represents a plane stress problem adopted in Rixen and Farhat (1997) in their study of preconditioners

Table 2. Eigenvalues of horizontal element 2 from inverse identified elemental flexibility

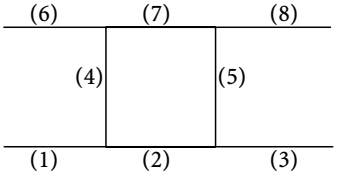

Mode	Exact	Initial	Iterated
Bending 1	1.6666E + 05	2.8992E + 05	1.6672E + 05
Bending 2	5.2000E + 05	4.8771E + 05	5.2000E + 05
Axial	2.0000E + 06	2.0011E + 06	2.0000E + 06

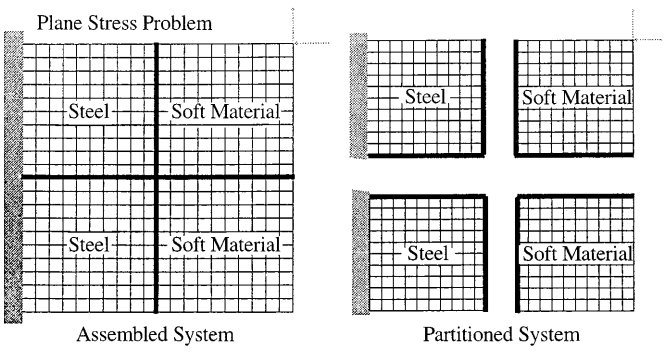

Fig. 11. Plane stress problem with material heterogeneity

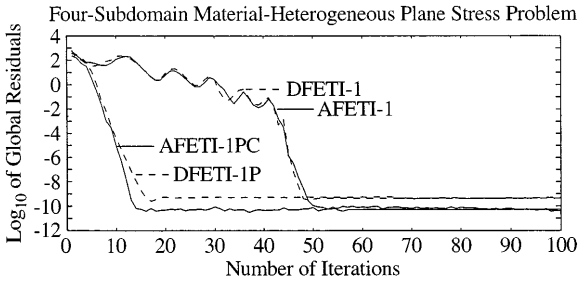

Fig. 12. Plane stress problem with material heterogeneity

for accelerating the iterative solution by parallel algorithms when the problem consists of material heterogeneities. Note that the partition boundaries are marked in Fig. 11 by bold lines. It should be noted that this problem can be used to test not only the parallel solution algorithm but also for the efficiency of contact enforcement as both problems must solve for the interface forces acting along the partition boundaries. The material heterogeneity is chosen such that the ratio of Young's moduli of steel and the soft material is 4096.

Figure 12 reports on the effect of the present flexibility normalization vs. the case without normalization ($\mathbf{D} = \mathbf{I}$) employing the present localized λ-method designated as AFETI-1PC and the AFETI-1 method, respectively. Included in the same figure is the performance of the preconditioning scheme of Rixen and Farhat (1997) in conjunction with the DFETI-1 method (Farhat and Roux, 1991; Farhat et al., 1994) designated herein as the DFETI-1P method. Note the marked improvement both by the present flexibility-normalized (AFETI-1PC) and the Rixen and Farhat preconditioning (DFETI-1P) schemes. This demonstrates that the present flexibility normalization offers a similar beneficial effect on iteration acceleration as that rendered by the preconditioning scheme of Rixen and Farhat (1997), thus confirming the analytical comparison offered in (49)–(51).

7.4
Partitioned 40-bay tower problem

Whereas the plane stress problem analyzed is to assess the performance of the flexibility normalization for material heterogeneities, the 40-bay tower problem shown in Fig. 14 is chosen for its robustness in handling geometric heterogeneities. The tower consists of 40 bays, with each bay made of 14 beam elements. For the present numerical experiments, two partitions are utilized: element-by-element partition leading to 560 substructures and bay-by-bay partition with a total of 40 substructures. It is noted that a significant coupling of axial and bending is effected at each joint, thereby causing stiffness mismatch.

Observe from Fig. 14 that both the AFETI-1 and the DFETI-1 methods perform relatively similar. When the flexibility normalization is invoked, that is, by using AFETI-1PC a marked improvement (13 vs. 73 iterations) is achieved.

It is found that DFETI-1 with the Rixen and Farhat preconditioning scheme, labeled as the DFETI-1P method, does not improve over the DFETI-1 method. As for the marked performance improvement of the present flexibility normalization strategy, we offer the following reasoning.

Observe that the AFETI-1PC projector $\mathbf{P}_\ell$ given by (51) incorporates the flexibility normalization whereas the DFETI-1P projector $\mathbf{P}_{\rm cl}$ does not account for the heterogeneity preconditioning. This difference, of course, is dramatic for this problem as geometric hetrogeneities are severe and everywhere along the partition boundaries. This aspect is further examined by solving a heterogeneous plate problem.

7.5
Cantilever heterogeneous plate under quasi-static uniform load

Finally, the present quasi-static algorithm summarized in (44) will be evaluated in solving a plate response problem as shown in Fig. 15. The plate is fixed at its left edge and

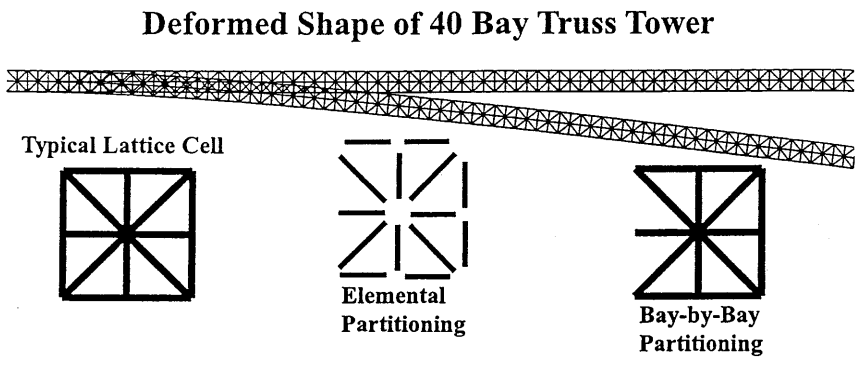

Fig. 13.
Cell dimension: 1×1 m
Area cross section: 0.01 m^2
Young's modulus: 690 GPa
Moment of inertia: 8.33×10^{-6} m^4

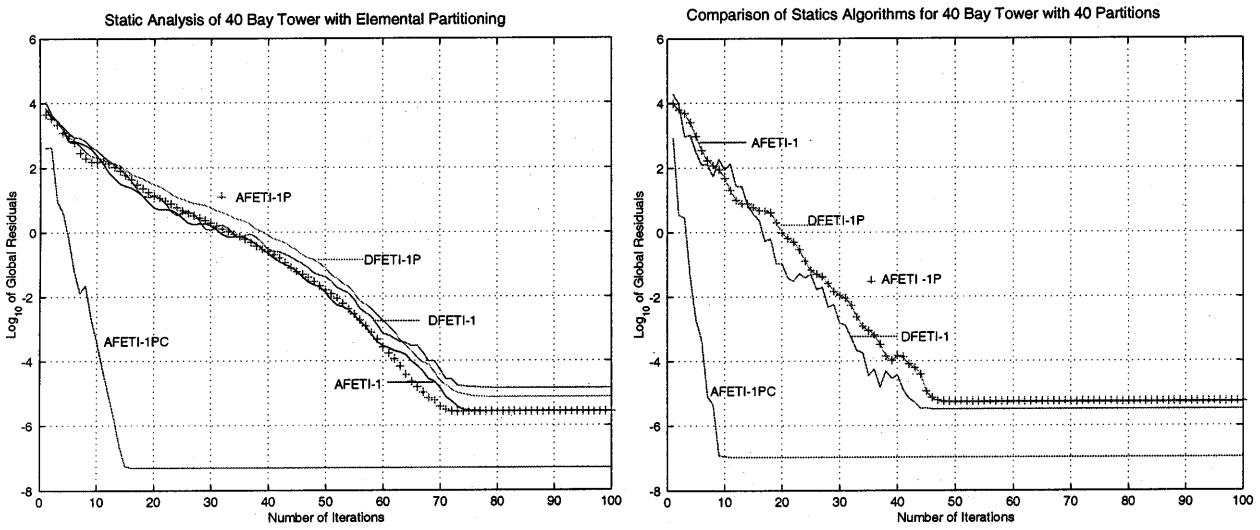

Fig. 14. Static analysis of 40 bay tower made of beam elements

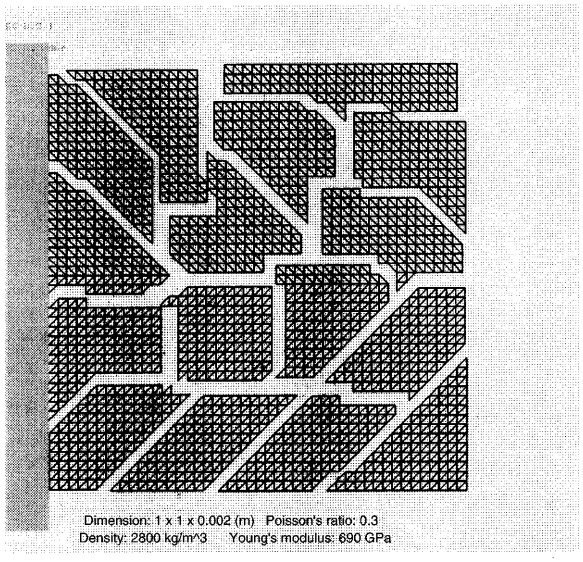

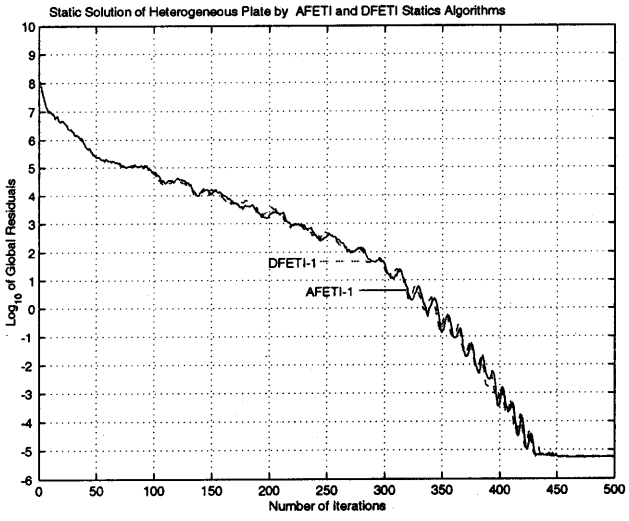

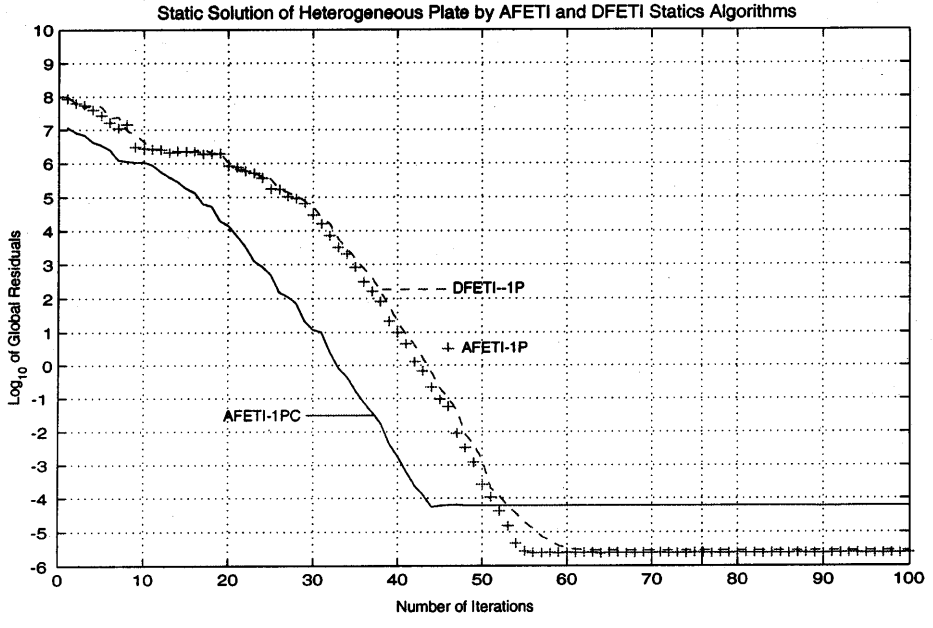

Fig. 15. Cantilieverd plate partitioned into 16 sub-structures

subjected to a uniform step load. An irregular 16-substructural partitioning is used for the present analysis. Material heterogeneities are introduced such that a pair of soft and hard partitions are alternatively assigned for the 16 partitions with their rigidity ratio of 4096. Included in the analysis is the DFETI-1 algorithm of Farhat and Roux (1991), Farhat et al. (1994) with and without the Rixen and Farhat heterogeneity preconditioner.

The performances of AFETI-1 and DFETI-1 are almost identical. When AFETI-1PC is employed, the iteration number is significantly reduced from 425 to 44. The DFETI-1P method that employs the preconditioning scheme of Rixen and Farhat (1997) also significantly reduced iterations from 425 to 52. For comparisons, the AFETI-1P algorithm that invokes the flexibility normalization only in the preconditioner but a standard projector, viz., $\mathbf{P}_\ell$ with $\mathbf{D} = \mathbf{I}$, was also used to solve the same problem. The result indicates that the AFETI-1P method yields an identical performance to that of the DFETI-1P method with the heterogeneous preconditioner. Hence, we conclude that the performance difference between the present flexibility normalized AFETI-1PC algorithm and the DFETI-1P algorithm with the heterogeneous preconditioner is primarily due to the projectors as can be seen in Table 1.

8 Conclusions

The present paper has presented a formalization of the localized λ-method that has been employed in the derivations of the partitioned equilibrium equations for structures (Park, Justino and Felippa, 1998a). The partitioned equilibrium equations and their specializations have been applied to parallel computations (Park, Justino and Felippa 1997; Felippa and Park, 1997), inverse problems (Alvin and Park, 1996; Park, et al., 1997; Park and Felippa, 1998b), structural system identification (Park and Reich, 1998), and localized active vibration control (Park and Kim, 1998).

It is shown that the localized λ-method circumvents the non-uniqueness issues associated with the classical λ-method for interface modeling where more than two nodes are constrained.

The flexibility normalization presented in Sect. 4 offers beneficial effects for partitioned analysis and contact enforcement. In particular, it accelerates substantially the iterative convergence for both material and geometric heterogeneities. Although not elaborated herein, the contact interface estimation formula (28) may offer a rational basis for detecting contact interfaces.

Encouraged by the usefulness of the localized λ-method for applications cited so far, the method is now being evaluated for contact-impact problems and sensitivity derivations of design parameters in optimization via partitioned approaches.

References

Argyris JH, Kelsey S (1960) Energy theorems and structural analysis, Buttersworth, London, reprinted from Aircraft Engrg. 26, Oct–Nov 1954 and 27, April–May 1955

Alvin KF, Park KC (1996) Extraction of substructural flexibility from measured global frequencies and mode shapes, Proc. 1996 AIAA SDM Conference, Paper No. AIAA 96-1297, April 15–19 1996, Salt lake City, Utah. Submitted to AIAA J. in 1999

Denke PH (1962) A general digital computer analysis of statically indeterminate structures, NASA Tech. Note D-1366

Dugas, Réne (1988) A history of mechanics, pp. 332–338, Dover, New York

Farhat C, Roux F-X (1991) A method of finite element tearing and interconnecting and its parallel solution algorithm. Int. J. Num. Meth. Eng. 32:1205–1227

Farhat C, Crivelli L, Roux F-X (1994) A transient FETI methodology for large-scale implicit computations in structural mechanics, Int. J. Num. Meth. Eng. 37:1945–1975

Farhat C, Roux F-X (1994) Implicit parallel processing in structural mechanics. Comput. Mech. Advances 2:1–124

Felippa CA (1987) Will the force method come back? J. App. Mech. 54:728–729

Felippa CA, Park KC (1980) Staggered transient analysis procedures for coupled-field mechanical systems: formulation. Comp. Meth. Appl. Mech. Eng. 24:61–111

Felippa CA, Park KC (1997) A direct flexibility method, Comp. Meth. Appl. Mech. Eng., 149:319–337

Gallagher RH (1987) Private communication to K.C. Park

Gumaste UA, Park KC, Alvin KF (1998) A simple implicit partitioned solution procedure for parallel analysis of structural dynamic systems, Center for Aerospace Structures, Report No. CU-CAS-98-21, University of Colorado, Boulder, CO, November 1998

Haug EJ (ed) (1984) Computer aided analysis and optimization of mechanical system dynamics, Springer-Verlag, Berlin

Justino MR Jr., Park KC, Felippa CA (1997) An algebraically partitioned FETI method for parallel structural analysis: implementation and numerical performance evaluation, Int. J. Num. Meth. Eng. 40:2739–2758

Kaneko I, Lawo M, Thierauf G (1982) On computational procedures for the force method. Int. J. Num. Meth. Eng. 18:1469–1495

Lagrange JL (1788) Mechanique analytique, reprinted by Gauthier-Villars, Paris, 1888

Lanczos C (1970) The variational principles of mechanics, Univ. of Toronto Press, 4th ed., Toronto, Canada, pp. 141–147

Likins PW (1970) Dynamics and control of flexible space vehicles, NASA TR-32-1329

Mach E (1960) The science of mechanics, Open Court Pub. Co., La Salle, Illinois, pp. 560–577

Park KC (1980) Partitioned transient analysis procedures for coupled-field problems: stability analysis. J. Appl. Mech. 47:370–376

Park KC, Justino MR Jr., Felippa CA (1997) An algebraically partitioned FETI method for parallel structural analysis: algorithm description. Int. J. Num. Meth. Eng. 40:2717–2737

Park KC (1998) A contact algorithm based on localized Lagrangian multipliers for partitioned parallel computations, Center for Aerospace Structures, Report No. CU-CAS-98-15, University of Colorado, Boulder, CO, July 1998

Park KC, Kim, Nag-In (1998) A localized vibration control based on partitioned flexibility method, part I: theory, Center for Aerospace Structures, Report No. CU-CAS-98-13, University of Colorado, Boulder, CO, July 1998

Park KC, Reich GW, Alvin KF (1997) Damage detection using localized flexibilities, in Chang, F-K. (ed): Structural Health Monitoring, Current Status and Perspectives, Technomic Pub., 1997, pp. 125–139

Park KC, Reich GW (1998) A theory for strain-based structural system identification, Proc. Nineth International Conference on Adaptive Structures and Technologies, Cambridge, MA, Oct. 14–16, 1998

Park KC, Felippa CA (1998a) A variational framework for solution method developments in structural mechanics. J. App. Mech. March 1998, 65/1:242–249

Park KC, Felippa CA (1998b) A flexibility-based inverse algorithm for identification of structural joint properties, to appear in ASME Symposium on Computational Methods on Inverse Problems, November 1998, Anaheim, CA

Patnaik SN (1973) An integrated force method for discrete analysis. Int. J. Num. Meth. Eng. 6:237–251

Przemieniecki JS (1968) Theory of matrix structural analysis, McGraw-Hill (Dover edition 1986, New York)

Richter SL, Collins EG Jr (1989) A homotopy algorithm for reduced-order controller design using the optimal projection equations, Proceedings of the Conference on Decision and Control, Dec. 1989, Tampa, FL, pp. 506–511

Rixen D, Farhat C (1997) A simple and efficient extension of a class of substructure based preconditioners to heterogeneous structural mechanics problems, Center for Aerospace Structures, Report CU-CAS-97-18, University of Colorado at Boulder, December 1997

Routh EJ (1905) Dynamics of a system of rigid bodies: elementary part, Macmillan Co., London, pp. 317–323